



## Bias-tuned reduction of self-absorption in polymer blend electroluminescence

B. Ruhstaller<sup>a</sup>, J.C. Scott<sup>b</sup>, P.J. Brock<sup>b</sup>, U. Scherf<sup>c</sup>, S.A. Carter<sup>a,\*</sup>

<sup>a</sup> *University of California Santa Cruz, Physics Department, Santa Cruz, CA 95064, USA*

<sup>b</sup> *IBM Almaden Research Center, San Jose, CA 00000, USA*

<sup>c</sup> *Max-Planck-Institut für Polymerforschung, D-55021 Mainz, Germany*

Received 21 June 1999; in final form 2 December 1999

### Abstract

We present a concentration- and bias-dependent electroluminescence study on MEH-PPV aggregation in a binary polymer blend with the blue-emitting Me-LPPP as host. In low-concentration blends the spectral features of MEH-PPV peak at 560 nm, identical to its photoluminescence spectrum in dilute solution, and therefore suggesting effective hindering of aggregation-induced self-absorption. At higher concentrations the electroluminescence spectra are dominated by MEH-PPV peaking at 600 nm and a dramatic shift of spectral weight to the 560 nm peak is observed with increasing bias. We attribute this novel effect to a reduction of self-absorption caused by either photo- or charge-induced bleaching. © 2000 Elsevier Science B.V. All rights reserved.

### 1. Introduction

Further insight into the discrepancy between photoluminescence quantum efficiencies achieved from the same polymer in solution and in pure film [1–4] is required in order to improve the electroluminescence quantum efficiency. Aggregate formation plays a key role and can be observed as spectral changes in both absorption and emission. We shall use the term ‘aggregation’ to describe partially aligned polymer chains that interact and allow for a more delocalized excited state complex with absorption and emission red-shifted with respect to the single-chain species [1–3,5]. It was found in photophysics studies [1,2] that the excited state lifetimes of aggregation states

are significantly longer than those of single-chain species and therefore prevent fast radiative decay required for efficient luminescence. Moreover, a reduction of aggregate induced self-absorption is highly desirable for lowering the threshold for amplified spontaneous emission. These issues can be studied most directly by means of electroluminescence of polymer blends.

Blend systems so far have mainly been investigated to demonstrate efficient energy transfer from the host to a low-concentration guest [6–9]. In most cases small organic molecules or dye molecules have been used as dopants and the concentration of the guest was kept low to avoid luminescence quenching [3]. Concentration dependence has been studied to achieve color tuning and efficient white light [6,10,11]. In addition, the threshold for amplified spontaneous emission was demonstrated to decrease

\* Corresponding author. Fax: +1-831-459-3043; e-mail: sacarter@cats.ucsc.edu

in a polymer blend system due to reduced self-absorption [12].

Electroluminescence (EL) of single-layer polymer light-emitting diodes (PLEDs) exhibits no change in emission spectrum as a function of applied bias if heating effects [13] are excluded. In previous studies of blend systems, only the amplitudes of the spectral features of individual constituents but not the amplitudes of individual vibronic transitions were found to vary as a function of bias [14,15]. The blend system presented here is distinguished by very efficient electroluminescence of its constituent conjugated polymers [16–18]. Therefore, in blends of finite ratios one expects a competition of electroluminescence of the two polymers. In addition, these polymers represent a symmetric microjunction since the band gap of MEH–PPV lies within the band gap of Me-LPPP. In small blend ratios one would expect both efficient energy and charge transfer to MEH–PPV; however, we find a bias-tuned redistribution of spectral weight for an intermediate blend ratio which cannot be described solely by energy and charge transfer nor phase separated polymer domains [15,19,20].

## 2. Experimental

The blend solutions are prepared by mixing the two solutions of 1 wt% polymer in *p*-xylene and ultrasonicated the solution thereafter. The solution is spun cast onto an ITO patterned glass substrate covered with the conducting polymer PEDT [16]. After evaporation of the solvent, Ca cathodes and a protecting layer of Al are evaporated on top. The active layer thickness is 100 nm. All measurements are carried out in a nitrogen atmosphere at room temperature. We use an OceanOptics grating spectrometer to acquire the spectrum as a function of applied bias. Radiance and luminance units have been calibrated against a He lamp using an integrating sphere. To reduce heating effects and allow for current densities up to 2 A/cm<sup>2</sup>, we operate at a duty cycle of 5% and measure the current with a lock-in amplifier. Polymer film absorption was determined by measuring reflectivity and transmission with an optical thin-film analyzer from n&k Technologies. The photoluminescence spectrum of the dilute MEH–PPV: *p*-xylene solution was measured

using a halogen lamp whose beam was in normal incidence relative to the spectrometer detection fiber.

## 3. Results and discussion

### 3.1. Polymer blends: absorption and emission spectra

MEH–PPV and Me-LPPP are widely used efficient conjugated polymers with band-gap energies of 2.4 and 2.7 eV, respectively. Me-LPPP has a LUMO level of 2.8 eV and a HOMO level of 5.5 eV [21] whereas the levels for MEH–PPV are 2.95 and 5.35 eV, respectively [22]. Due to this symmetric alignment, Förster-type energy transfer [9] and bipolar charge transfer from Me-LPPP to MEH–PPV can occur. Fig. 1 shows their absorption and electroluminescence spectra for pure and blend films. Films of

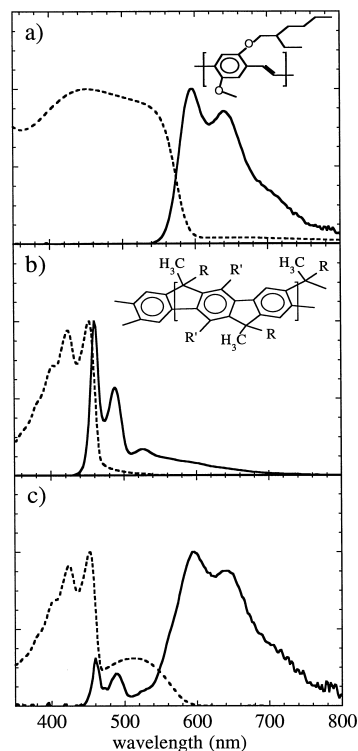


Fig. 1. Normalized absorption (dashed) and electroluminescence (continuous) spectra: (a) MEH–PPV; (b) Me-LPPP; and (c) 8 wt% MEH–PPV:Me-LPPP blend. Inset: chemical structure, where  $R = 1,4\text{-C}_4\text{H}_6\text{-C}_{10}\text{H}_{21}$  and  $R' = \text{C}_6\text{H}_{13}$ .

the ladder-type polymer Me-LPPP exhibit a smaller Stokes shift and sharper vibronic features than MEH-PPV. The MEH-PPV film shows less vibronic structure in both absorption and emission.

For the 10 wt% MEH-PPV:Me-LPPP blend in Fig. 1c) we find the main absorption and emission bands well separated by 100 nm and therefore a reduction of self-absorption. While the absorption is dominated by Me-LPPP, the emission is dominated by MEH-PPV. All electroluminescence spectra in Fig. 1 are taken at a bias of 8 V.

### 3.2. Electroluminescence performance: luminance vs. bias

A standard single-layer PLED configuration with an ITO/PEDT anode and a Ca cathode was used to investigate the electroluminescence performance of the pure and blend devices. The electrode work functions (ITO/PEDT: 5.1 eV, Ca: 2.9 eV) form nearly ohmic contacts with MEH-PPV as well as Me-LPPP. Due to the larger band gap however, the ‘turn-on’ voltage of Me-LPPP, 2.5 V, is slightly higher than the one of MEH-PPV with 1.8 V, as can be seen in the inset to Fig. 2. Both pure devices achieve a high brightness on the order of  $10^3$  cd/m<sup>2</sup> below 6 V bias. In blend devices one expects a competition of electroluminescence among the two polymers. The 8% blend device has an intermediate ‘turn-on’ voltage and achieves similar brightnesses at a slightly higher bias. Its overall power efficiency upon ‘turn-on’ is 0.3 lm/W. At a bias of 14 V, the color coordinates for this device are 0.35/0.36 and therefore very close to white. White emission can also be achieved at lower bias by choosing a lower blend ratio. The maximum external quantum efficiencies are 1.5% (MEH-PPV) and 1% (Me-LPPP and Blend).

### 3.3. Moderate concentration blend electroluminescence: bias-tuned reduction of self-absorption

We observe dramatic changes in the emission spectrum as a function of applied bias for a 10 wt% blend device, as shown in Fig. 3b. Upon ‘turn-on’, the device emits with a spectrum dominated by MEH-PPV. The spectral features of the MEH-PPV contribution are identical to the ones observed in

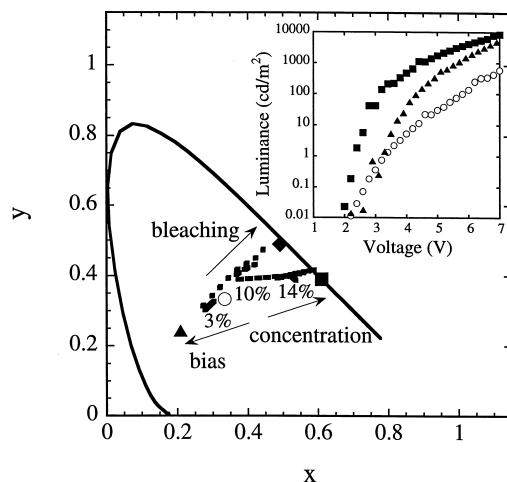


Fig. 2. Brightness plotted vs. voltage for pure (squares: MEH-PPV, triangles: Me-LPPP) devices and a 8% MEH-PPV:Me-LPPP blend (circles) device. The ‘turn-on’ voltages vary from 1.8 V (MEH-PPV) to 2.5 V (Me-LPPP). Brightnesses on the order of  $10^3$  cd/m<sup>2</sup> are achieved below 6 V. In the inset the colors seen by the human eye are quantified with CIE color coordinates. As a function of blend ratio and bias one achieves all colors including white (circle) lying within the triangle defined by MEH-PPV film (square, 0.61/0.39), Me-LPPP film (triangle, 0.2/0.24) and MEH-PPV dilute solution PL (diamond, 0.5/0.5).

pure MEH-PPV devices (see Fig. 1a) with a dominant peak at 600 nm and a sidepeak at 650 nm. With increasing bias the Me-LPPP contribution is increased significantly. Along with that an additional peak centered at 560 nm is developing and the sidepeak at 650 nm is decreasing. This transition is gradual and reversible.

The spectral changes are observed by the human eye as a color change from orange to white to greenish white. In the inset of Fig. 2 the emission colors are characterized quantitatively with CIE chromaticity coordinates. The points lying within the diameter of the surrounding line on this color coordinate plot represent colors detectable by the human eye. The coordinates  $x$  and  $y$  represent the red and green component, respectively, whereas the bluest color is represented by the point closest to the origin. While the large points specify the pure polymer color coordinates, the lines represent up and down sweeps in bias. We note that the high blend ratio bias sweep follows the connecting line between pure Me-LPPP blue and the pure MEH-PPV orange film

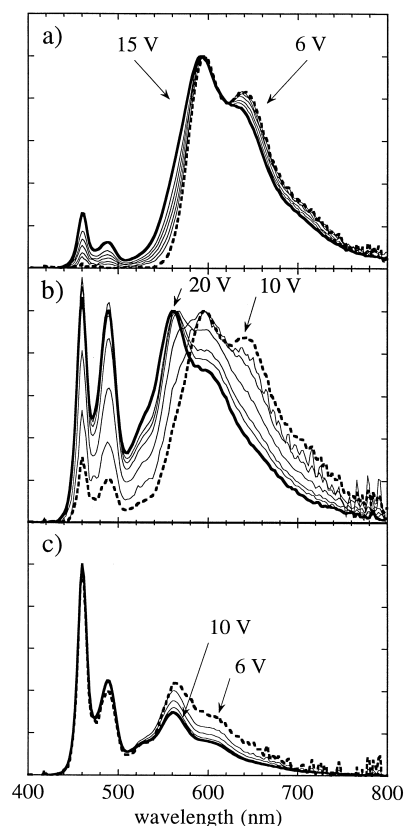


Fig. 3. Normalized EL spectra vs. bias. (a) High concentration (20 wt% MEH-PPV:Me-LPPP) blend. For increasing bias slight spectral changes at the sidepeak are observed. (b) Intermediate concentration (10 wt%) blend. A significant shift of spectral weight from the 600 nm to the 560 nm emission band for higher bias is observed. (c) Low concentration (3 wt%) blend. The spectral features of MEH-PPV are dominated by the 560 nm peak and decrease relative to the Me-LPPP peak emission for increasing bias.

emission whereas the low blend ratio bias sweep lies on the connecting line between pure Me-LPPP film blue and the yellow-green MEH-PPV dilute solution photoluminescence. The occurrence of the 560 nm peak in the intermediate blend ratio case is reflected as a curve toward the dilute solution photoluminescence color. The observed small hysteresis is subject of further investigations.

### 3.4. Analysis: vibronic structure

In conjugated polymers, typically two vibronic features in both emission and absorption can be

resolved, and assigned to the 0–0 and to the 0–1 vibronic transition. The first digit specifies the vibronic level of the excited singlet state and the second digit the vibronic level of the excited ground state (Fig. 4b). The amplitude of the vibrational peaks is given by the occupation numbers and the wavefunction overlap (Franck–Condon factor) of the vibronic levels involved. In contrast to the sharp vibronic features, interchain interactions are manifested as broad red-shifted emission features and can result from high concentration, poor solvent quality [1–3] or electrical and UV degradation [5]. In a pure Me-LPPP EL experiment with high current densities exceeding  $2 \text{ A/cm}^2$ , we find a decreasing 0–0 vibronic peak amplitude and a broad emission band at 550 nm [23], attributed to aggregate formation due to electrical degradation that is well distinguished from the sharp feature at 560 nm described in Section 3.3.

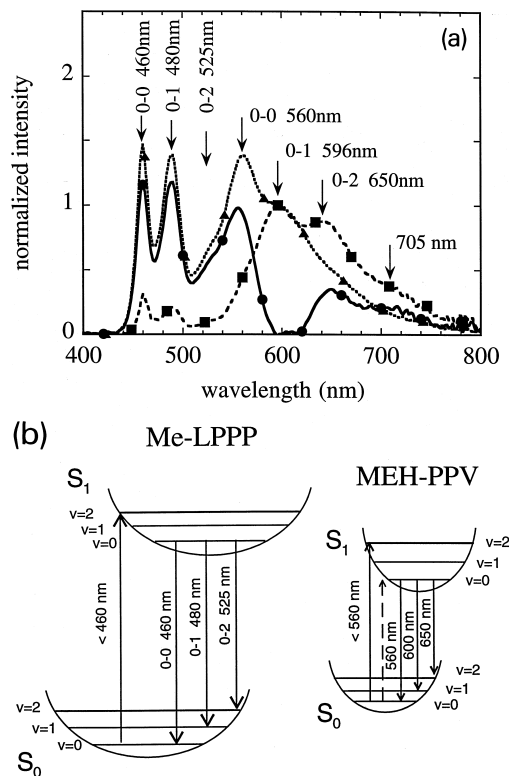


Fig. 4. EL spectra of the 10 wt% blend device for 10 V (squares) and 20 V (triangles) applied bias normalized at 600 nm and difference thereof (circles). (a) Labeled with the vibrational transitions as illustrated with the molecular energy level scheme (b). The dashed arrow in (b) represents aggregate absorption.

In Fig. 4a, the low-bias (10 V) and high-bias (20 V) EL spectra are normalized at 600 nm for comparison. The differential spectrum reveals the 560 nm peak and a reduced emission band above 650 nm. We assign the 560 nm peak to the 0–0 vibronic transition<sup>1</sup> of MEH–PPV and argue that this transition is self-absorbed in pure films due to aggregates. We note that this emission band is well separated from the Me-LPPP 0–2 vibronic transition at 525 nm. Since the 560 nm emission band appears in both low-concentration-blend EL and in dilute-solution PL (see Section 3.5), it cannot be assigned to an exciplex either. The simultaneous decrease of the red shoulder and increase of the 560 nm emission band suggests this transition to be solely originating from one species. The absorbing species are aggregates that have a red-shifted absorption below 600 nm and a broad emission band above 650 nm. We assign these features to aggregates and not to excimers, since the emission features are accompanied by a shift of the absorption edge, see Fig. 1a and c).

We believe this species to be bleached at high bias either due to the intense blue host emission or due to charge-induced absorption changes [24,25]. The first explanation requires the assumption of a blue radiant intensity within the device that is comparable to the intensities used to externally excite a photobleaching band in an equivalent polymer blend film [8]. We note that this photobleaching band was found to be significantly longer lived in the polymer blend than in the pure polymer film [8]. The second explanation is based on the non-negligible excited state absorption to the red part of the spectrum in the presence of high electrical excitation [24,25]. However, the substitution of the Me-LPPP host with the non-emissive polystyrene at a blend ratio of 8% exhibits an electroluminescence spectrum dominated at 600 nm which experiences only a minor blue-shift on the order of 5 nm for increasing bias [26]. Moreover, by decreasing the blend ratio of MEH–PPV in the polystyrene host to 0.2% we find a dominating

electroluminescence peak at 560 nm. This observation further implies that the 560 nm peak does not originate from the Me-LPPP host, but from the MEH–PPV itself.

Another possible explanation regards the distribution of the recombination zone within the electrodes which is in general nonuniform [27]. To investigate this explanation we fabricated a semitransparent device with a 3 nm thick Al cathode. Measuring the bias-dependent spectra from the cathode side, we found the same transition from the 600 nm to the 560 nm dominated emission peak of MEH–PPV at comparable bias. Therefore, it must be a bulk effect within the active layer, and the distribution of the recombination zone plays a minor role.

If we analyze the variation with bias of the individual peak intensities of MEH–PPV in the 10% blend device, we find no dramatic change but an overall brightness increase proportional to the Me-LPPP peak intensity that is accompanied by an exchange of MEH–PPV peak amplitudes. The discussion of MEH–PPV efficiency changes due to aggregation is complicated by the presence of efficient blue host emission. For all investigated concentrations, we find external quantum efficiencies of 1%, which is slightly lower than for the case of pure MEH–PPV (1.5%). This efficiency is limited by the host polymer.

### 3.5. Concentration dependence: consistency with dilute solution photoluminescence

Blends of either of the two extremes in concentrations do not exhibit the transition to the 560 nm peak discussed above. In the case of high concentration (Fig. 3a), the operating current regime is not sufficient to excite the transition. The emission spectra is dominated by an aggregated MEH–PPV species peaking at 600 nm with a tendency for the transition clearly visible for higher biases at the 650 nm side-peak and on the lower-wavelength side of the spectrum.

In the case of low concentration (Fig. 3c) the MEH–PPV spectral features are dominated at 560 nm and do not further change their shapes for increasing bias. We only observe an increasing contribution of Me-LPPP emission. Since the MEH–PPV

<sup>1</sup> We cannot exclude the existence of an additional vibronic transition at even higher energy, but still below the HOMO/LUMO gap of 2.4 eV [22]. For the purpose of this Letter though, we consider the 560 nm transition as the vibronic transition of highest energy.

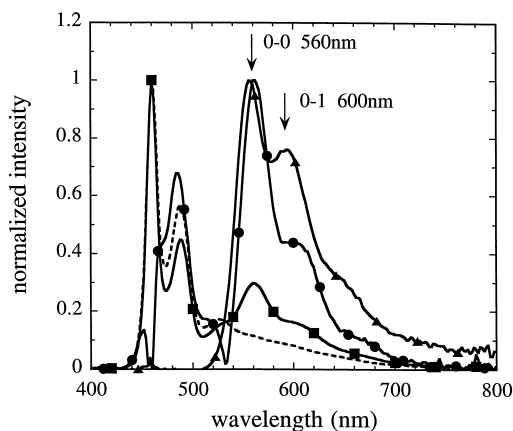


Fig. 5. Dilute (3 wt%) blend film EL spectrum at 10 V (squares) compared to dilute solution (0.5 wt%) PL spectrum (triangles). A normalized MEH–PPV spectrum (circles) is extracted from the blend EL by subtracting the Me-LPPP spectrum (dashed line).

polymer chains are well dispersed for the low concentration blend, Förster-type energy transfer can occur; however, concurrently the host shows efficient electroluminescence.

It is interesting to extract an MEH–PPV spectrum from the low-concentration-blend EL by deducting a normalized Me-LPPP EL spectrum (see Fig. 5). We measure a spectrum identical to the one found in dilute solution (0.5 wt% in *p*-xylene) photoluminescence. The discrepancy at the 650 nm emission band is attributed to an unequal degree of aggregation.

Our results on concentration dependent aggregation of MEH–PPV in the blend are in good agreement with nanoparticle composite PLEDs, where we observe a spectral blue-shift for increased nanoparticle concentration [26]. The importance of self-absorption can also be seen in pure Me-LPPP film samples themselves. The amplitude ratio of the first to second vibronic peak of Me-LPPP photoluminescence is reduced by self-absorption upon stacking of thin-film samples.

#### 4. Conclusions

Our results on concentration-dependent electroluminescence spectra of MEH–PPV blended into Me-LPPP demonstrate spectral features consistent with dilute solution photoluminescence in the case of low

concentration and with pure films in the high concentration case. For intermediate blend ratios ( $\sim 10$  wt%) and increasing bias we observe the development of an emission peak centered at 560 nm, which we assign to the 0–0 vibronic transition of MEH–PPV, along with a reduced red-shifted emission. Our results are interpreted in terms of an aggregation species of MEH–PPV with red-shifted absorption and emission. This species is responsible for self-absorption of the 0–0 vibronic transition at 560 nm of MEH–PPV. We attribute the observed reduction in self-absorption to photo- or charge-induced bleaching. As a result, we demonstrate efficient concentration- and bias-tuned colors including white and greenish white.

#### Acknowledgements

The authors acknowledge financial support from NSF GOALI Grant No. DMR 9704177. B.R. is thankful to the Sunburst Fonds ETH. We would like to thank n&k Technologies for providing the n&k thin-film analyzer.

#### References

- [1] T.-Q. Nguyen, V. Doan, B.J. Schwartz, *J. Chem. Phys.* 110 (1999) 4068.
- [2] R. Jakubiak, C.J. Collison, W.C. Wan, L.J. Rothberg, *J. Phys. Chem. A* 103 (1999) 2394.
- [3] J.H. Hsu, W. Fann, P.H. Tsao, K.R. Chuang, S.A. Chen, *J. Phys. Chem. A* 103 (1999) 2375.
- [4] S. Blumstengel, I. Sokolik, R. Dorsinville, D. Voloschenko, M. He, O. Lavrentovich, L.-C. Chien, *Synth. Met.* 99 (1999) 85.
- [5] V. Bliznyuk, S.A. Carter, J.C. Scott, G. Klärner, R.D. Miller, D.C. Miller, *Macromolecules* 32 (1999) 361.
- [6] S. Tasch, E.J.W. List, C. Hochfilzer, G. Leising, P. Schlichting, U. Rohr, Y. Geerts, U. Scherf, K. Müllen, *Phys. Rev. B* 56 (1997) 4479.
- [7] V.G. Kozlov, V. Bulovic, P.E. Burrows, M. Baldo, V.B. Khalfin, G. Parthasarathy, S.R. Forrest, Y. You, M.E. Thompson, *J. Appl. Phys.* 84 (1998) 4096.
- [8] G. Cerullo, M. Nisoli, S. Stagira, S. De Silvestri, *Chem. Phys. Lett.* 288 (1998) 561.
- [9] Th. Förster, *Ann. Phys.* 2 (1948) 55.
- [10] S. Tasch, E.J.W. List, O. Ekstrom, W. Graupner, G. Leising, P. Schlichting, U. Rohr, Y. Geerts, U. Scherf, K. Müllen, *Appl. Phys. Lett.* 71 (1997) 2883.

- [11] E.J.W. List, L. Holzer, S. Tasch, G. Leising, U. Scherf, K. Müllen, M. Catellani, S. Luzzati, *Solid State Commun.* 109 (1999) 455.
- [12] R. Gupta, M. Stevenson, A. Dogariu, M.D. McGehee, J.Y. Park, V. Srdanov, A.J. Heeger, H. Wang, *Appl. Phys. Lett.* 73 (1998) 3492.
- [13] N. Tessler, N.T. Harrison, D.S. Thomas, R.H. Friend, *Appl. Phys. Lett.* 73 (1998) 732.
- [14] X.Z. Jiang, Y.Q. Liu, X.Q. Song, D.B. Zhu, *Synth. Met.* 91 (1997) 311.
- [15] M. Berggren, O. Inganäs, G. Gustafsson, J.C. Carlberg, J. Rasmussen, M.R. Andersson, T. Hjertberg, O. Wennerström, *Nature (London)* 372 (1994) 444.
- [16] S.A. Carter, J.C. Scott, P.J. Brock, *Appl. Phys. Lett.* 71 (1997) 1145.
- [17] S.A. Carter, M.S. Angelopoulos, P.J. Karg, J.C. Brock, J.C. Scott, *Appl. Phys. Lett.* 70 (1997) 2067.
- [18] V. Bliznyuk, B. Ruhstaller, P.J. Brock, U. Scherf, S.A. Carter, *Adv. Mater.* (to be published).
- [19] J.H. Hsu, P.K. Wei, W.S. Fann, K.R. Chuang, S.A. Chen, *Ultramicroscopy* 71 (1998) 263.
- [20] K. Dalnoki-Veress, J.A. Forrest, J.R. Dutcher, *Phys. Rev. E* 57 (1998) 5811.
- [21] S. Tasch, A. Niko, G. Leising, U. Scherf, *Appl. Phys. Lett.* 68 (1996) 1090.
- [22] I.H. Campbell, T.W. Hagler, D.L. Smith, J.P. Ferraris, *Phys. Rev. Lett.* 76 (1996) 1900.
- [23] U. Lemmer, S. Heun, R.F. Mahrt, U. Scherf, M. Hopmeier, U. Siegner, E.O. Göbel, K. Müllen, H. Bässler, *Chem. Phys. Lett.* 240 (1995) 373.
- [24] M. Redecker, H. Bässler, *Appl. Phys. Lett.* 69 (1996) 70.
- [25] N. Tessler, D.J. Pinner, V. Cleave, D.S. Thomas, G. Yahioglu, P. Le Barny, R.H. Friend, *Appl. Phys. Lett.* 74 (1999) 2764.
- [26] B. Ruhstaller, J.C. Scott, P.J. Brock, U. Scherf, S.A. Carter, *Appl. Phys. Lett.* (submitted).
- [27] G.G. Malliaras, J.C. Scott, *J. Appl. Phys.* 83 (1998) 5399.